Wu, Z., Yin, Q., Guo, Z. et al. Comparison of Arctic and Southern Ocean sea ice between the last nine interglacials and the future. Clim Dyn (2022). https://doi.org/10.1007/s00382-022-06140-4

Insolation and CO_2 induced variations in the sea ice of the last nine interglacials and their comparison with the present and future

Zhipeng Wu[1,2,3*], Qiuzhen Yin[2*], Zhengtang Guo[1,3,4], André Berger[2]

[1]Key Laboratory of Cenozoic Geology and Environment, Institute of Geology and Geophysics, Chinese Academy of Sciences, Beijing, China

[2]Georges Lemaître Center for Earth and Climate Research, Earth and Life Institute, Université catholique de Louvain, Louvain-la-Neuve, Belgium

[3]University of Chinese Academy of Sciences, Beijing, China

[4]CAS Center for Excellence in Life and Paleoenvironment, Beijing, China

*Corresponding authors: Zhipeng Wu (zhipeng.wu@uclouvain.be), Qiuzhen Yin (qiuzhen.yin@uclouvain.be)

Abstract

Understanding the sea ice variability and the mechanisms involved during warm periods of the Earth is essential for a better understanding of the sea ice changes at the present and in the future. Based on simulations with the model LOVECLIM, this study investigates the sea ice variations during the last nine interglacials and focuses on the inter-comparison between interglacials as well as their differences from the present and future. Our results show that the annual mean Arctic sea ice variation is primarily controlled by local summer insolation, while the annual mean Southern Ocean sea ice variation is more influenced by the CO_2 concentration but the effect of local summer insolation can't be ignored. The lowest Arctic sea ice area results from the highest summer insolation at MIS-15, and the lowest Southern Ocean sea ice area at MIS-9 is explained by the highest CO_2 concentration and moderate local summer insolation. As compared to the present, the last nine interglacials all have much less sea ice in the Arctic annually and seasonally due to high summer insolation. They also have much less Arctic sea ice in summer than the double CO_2 experiment, which makes to some degree the interglacials possible analogues for the future. However, compared to the double CO_2 experiment, the interglacials all have much more sea ice in the Southern Ocean due to their much lower CO_2 concentration, which excludes the possibility of the interglacials as analogues for the future in the Southern Ocean. Our results suggest that in the search for potential analogues of the present and future climate, the seasonal and regional climate variations should be considered.

Keywords: Sea ice, Interglacials, Insolation, Arctic, Southern Ocean, CO_2, Paleoclimate modeling

1. Introduction

Sea ice is an important component of the polar and global climate system, in part, due to its high albedo and low thermal conductivity, which are associated with the temperature-albedo feedback and the thermal insulation effect. It normally amplifies the climate variability at high latitudes, often known as polar amplification (e.g. Serreze and Barry 2011). In addition, the melting and formation of sea ice can change the oceanic salinity structure. When sea ice forms, brine is rejected towards the ocean, suppling dense and well ventilated water to the global intermediate/deep water circulation, while it causes stratification between near-surface and deeper water during sea ice melts (Goosse et al. 2013). Sea ice also impacts the thermosteric sea level (e.g. sea level rise due to thermal expansion of the ocean) and the barystatic sea level (e.g. sea level rise due to fresh water input into the ocean) (Hobbs et al. 2016). Changes in sea ice extent not only affect the surface mass balance of the ice sheets (Krinner et al. 2007), but also shift the latitude of the mid-latitude storm tract belt (Kidston et al. 2011). Moreover, sea ice may influence the structure and function of high-latitude ecosystems and biogeochemical cycles (Delille et al. 2014), such as control the light and the distribution of phototrophic organisms, polar bear and penguin species (Ducklow et al. 2013).

Rapid sea ice changes in the Arctic and Southern Ocean are observed not only during the recent decades (e.g. Serreze et al. 2016; Turner et al. 2013), but also during past interglacial periods based on proxy reconstructions (e.g. Cronin et al. 2013; Wolff et al. 2006). Based on paleo sea ice proxies, Bennike (2004) found that there was more sea ice in Greenland than at present during the early-mid Holocene and less sea ice during late Holocene. Stein et al. (2017) suggested lower sea ice cover in the Arctic Ocean during the last interglacial relative to today. Due to the lack of suitable, high-resolution proxies and limitation in dating technique, most sea ice reconstructions focus on the very recent interglacials, such as Holocene (e.g. Vare et al. 2009; de Vernal et al. 2020) and the last interglacial (e.g. Stein et al. 2017). A few long sea ice reconstructions covering several glacial-interglacial cycles have been established using paleoclimate records in the Arctic (Polyak et al. 2010; Cronin et al. 2010, 2013, 2017) and in the Southern Ocean (Wolff et al. 2006). These studies show that a major shift towards perennial sea ice in western Arctic Ocean occurred after MIS-11 (Cronin et al. 2017), and most of the Arctic Ocean might have been free of summer ice cover during the last interglacial which were mainly attributed to high insolation intensity (Polyak et al. 2010; Cronin et al. 2013). Spectral analyses indicate that the Arctic sea ice variations contain strong precession and obliquity cycles, and with precession signals dominating (Cronin et al. 2013; Lo et al. 2018). In the Southern Ocean, proxy record indicates that the maximum sea ice extent at MIS-13 and the minimum sea ice extent during the last interglacial, and the sea ice variations show very strong 100 ka cycles (Wolff et al. 2006). Climate modeling has also been used to understand the sea ice variations during past interglacials, for instance, during the Holocene (Goosse et al. 2013; Otto-Bliesner et al. 2020), the last interglacial (Guarino et al. 2020; Otto-Bliesner et al. 2020, 2021; Kageyama et al. 2021), the MIS-13 (Wu et al. 2020) and the last nine interglacials (Yin and Berger 2012). These studies reveal that the Arctic and Southern Ocean sea ice variations show different characteristics under different interglacial conditions, and the dominating forcing mechanisms might be different.

Past interglacials, as the most recent warm periods in the Earth's history, play an important role in paleoclimate researches because they provide a basis for better understanding our present-day warm climate and its future evolution (Tzedakis et al. 2009; Past Interglacials Working Group of PAGES 2016). They are useful to better understand climate internal processes and related feedbacks during warm intervals, and to discuss the effect of different external drivers, such as insolation and atmospheric CO_2 concentration (Yin and Berger 2012, 2015). In addition, past interglacials might provide analogues of the future climate under natural warm climate variability, and help to improve our estimate of the sensitivity of the climate system to different forcings, such as the increased atmospheric CO_2 concentration affected by anthropogenic processes. As far as the sea ice variations are concerned, questions can be raised on (1) what are the differences between interglacials and between Arctic and Southern Ocean sea ice variations during these warm periods, (2) what are the controlling forcing and mechanisms, and (3) how are the past interglacials different from the present and the future?

A preliminary investigation of the individual and combined effect of insolation and CO_2 on the climate of the last nine interglacials has been performed by Yin and Berger (2012) using model simulations and factor separation analysis. Based on the simulations performed in their study, here we make an in-depth analysis of the internal processes that control the interglacial sea ice variability, and focus on the inter-comparison between individual interglacials as well as their differences from the present and future.

2 Model and experiments design

The model used in this study is LOVECLIM, a three-dimension Earth system Model of Intermediate Complexity (Goosse et al. 2010). In our study, the atmosphere (ECBilt), the ocean and sea ice (CLIO) and the terrestrial biosphere (VECODE) are interactively coupled, and the ice sheets are fixed to the present situation. Detailed description of the model can be found in Goosse et al. (2010). In this study, we focus on the sea ice variations, thus we mainly address the CLIO component, which is made up of an ocean general circulation model coupled to a comprehensive thermodynamic-dynamic sea-ice model (Goosse and Fichefet 1999). Its horizontal resolution is 3° in longitude and latitude, and there are 20 levels in the ocean. LOVECLIM has been shown to have the ability to reproduce the major characteristics of climate changes for both present-day and some important past periods (see references in

Goosse et al. 2010). In addition, LOVECLIM has been demonstrated to simulate reasonably well the sea ice variations during the last millennium, the Holocene, the last Glacial Maximum, over the last 9000 years, over the past 130 ka, over the past 408ka, and during MIS-13, as compared with the proxy records and other many sophisticated general circulation models (Renssen et al. 2005a, 2005b; Goosse et al. 2013; Timmermann et al. 2014; Lo et al. 2018; Wu et al. 2020; Kageyama et al. 2021).

First, to investigate the combined effect of insolation and CO_2 on the sea ice of the last nine interglacials, the nine control experiments (f11) performed in Yin and Berger (2012) are used. In these control experiments, both insolation and CO_2 are taken at their interglacial levels, and details of experiments setup have been given in Yin and Berger (2012). Then, three new experiments were performed in our study to represent the present and future climate, in order to compare them with the interglacials. Two experiments are used to represent the present climate: one is the pre-industrial experiment (hereafter abbreviated as PI experiment) which could be considered as the present-day climate under the natural climate variability, its astronomical parameters are taken the values at 0 ka (Berger 1978), CO_2 = 280 ppmv, CH_4 = 760 ppbv, and N_2O = 270 ppbv; the other is a transient simulation from 1500 AD to 2000 AD in which the effect of the anthropogenic forcing is also included, and the last 30-year average climatology is analyzed (hereafter abbreviated as PD experiment). The CO_2 concentration is increased with time in the PD experiment, and the last 30-year average CO_2 concentration is 66 ppmv higher than the PI one (346 vs. 280 ppmv).

As the CO_2 concentration projected at the end of the 21th century is most likely much higher with the largest probability between 421 and 936 ppmv (IPCC 2014) and as a nearly ice-free Arctic Ocean in the summer sea ice minimum is projected for RCP8.5 (IPCC 2014), it would be interesting to see if sea ice conditions similar to projected for the future happened during the interglacials. In addition, the double CO_2 experiment (CO_2 doubled as compared to the PI) has become a standard experiment in climate science (Myhre et al. 2017), this CO_2 concentration being very close to the RCP4.5. In this study, we also performed a double CO_2 experiment to represent the future (hereafter abbreviated as PI_double experiment).

The equilibrium climate sensitivity is a key point in projecting future climate change (Cox et al. 2018; Nijsse et al. 2020), and it is defined as the global mean surface air temperature increase once radiative equilibrium is reached in response to the atmospheric CO_2 concentration twice the pre-industrial level (Hansen et al. 1984; Rugenstein et al. 2020). Before investigating the difference of sea ice between interglacials under the combined effect of insolation and CO_2 as well as their differences from the present and future, we have first analyzed the sensitivity of sea ice to CO_2 in our model, by calculating the decrease of sea ice area at equilibrium following a double CO_2 concentration, and compared our results with other models. Fig. 1 shows that the sensitivity of the global sea ice area in response to the double CO_2 concentration in LOVECLIM is at the medium level (5th) among the nine models (Fig. 1a). For the sensitivity of the Arctic sea ice area, LOVECLIM is at relative low level (Fig. 1b), but LOVECLIM is at high level for the sensitivity of the Southern Ocean sea ice area (Fig. 1c). Considering the three cases, CESM2 is the most similar with LOVECLIM among the nine models.

3. Results and discussion

3.1 Difference of sea ice area between interglacials and the impact of insolation and CO_2

Fig. 2a shows the simulated annual and seasonal Arctic sea ice area over the last nine interglacials in response to the combined effect of insolation and CO_2. MIS-15, MIS-9 and MIS-5 have the smallest annual mean sea ice area, MIS-13 has the largest one. The simulated winter Arctic sea ice area shows very small variation between the interglacials, and the variation in the annual mean is mainly explained by the variation in summer, which is similar to the recent observation (Titchner and Rayner 2014). MIS-15, MIS-9 and MIS-5 have the smallest summer Arctic sea ice area, MIS-13 has the largest one, which is the same as the annual mean results. Previous study showed that the variation of the Arctic sea ice in summer is dominated by local summer insolation (Yin and Berger 2012). MIS-15, MIS-9 and MIS-5 have the highest summer insolation (Fig. 3a), explaining their smallest sea ice area. On the contrary, MIS-13, MIS-7 and MIS-11 have the lowest summer insolation (Fig. 3a), explaining their largest sea ice area, while the large annual mean Arctic sea ice area at MIS-17 could probably be related to its lowest CO_2 concentration and moderate local summer insolation (Fig. 3b).

In the Southern Ocean, MIS-5, MIS-9 and MIS-11 have the smallest annual mean sea ice area, and MIS-13 and MIS-17 have the largest one (Fig. 2b). Both the simulated local summer and local winter sea ice area in the Southern Ocean show significant variations between the interglacials with the amplitude being larger in summer (Fig. 2b). Previous study showed that, in the Southern Ocean, CO_2 plays a dominant role in the sea ice variation in local winter, whereas both insolation and CO_2 play an important role on the sea ice in local summer (Yin and Berger 2012). This leads to a dominant role of CO_2 in the variation of the annual mean sea ice area in the Southern Ocean, but with a non-negligible role of insolation. The smallest annual mean Southern Ocean sea ice at MIS-5, MIS-9 and MIS-11 are explained by the highest CO_2 concentration (Fig. 3b) during these interglacials and a not very low local summer insolation (Fig. 3a). The largest annual mean Southern Ocean sea ice area at MIS-13 and MIS-17 are explained by the lowest CO_2 concentration (Fig. 3b) combined with the low local summer insolation (Fig. 3a). Our results show that both the annual mean Arctic and Southern Ocean sea ice area at MIS-19 is the closest to that at MIS-1 and is followed by MIS-11 (Fig. 2), which is in line with the proposition that MIS-19 is a better analogue for MIS-1 than MIS-11 (Tzekadis et al. 2012; Yin and Berger 2012, 2015). In addition, our results show that the Mid-Brunhes Event (MBE) (Yin and Berger 2010) appears to be significant in the Southern Ocean sea ice, which is characterized by less sea ice in MIS-1, -5, -7, -9 and -11 than in MIS-13, -15, -17 and -19, but it is not obvious in the Arctic sea ice. This can be explained by the fact that the Southern Ocean sea ice is mainly dominated by CO_2 which itself shows a clear MBE while the Arctic sea ice is mainly dominated by local summer insolation which does not have clear MBE (Yin and Berger 2012). The sea ice reconstruction in the Southern Ocean of Wolff et al. (2006) is one of the very few long sea ice reconstructions covering several glacial-interglacial cycles. Their results have a great consistency with our simulated results. Both the reconstructions and simulations show that MIS-13 and MIS-17 have the largest annual mean Southern Ocean sea ice and MIS-5 and MIS-9 have the smallest one (Fig. 4). A notable difference is in MIS-15 which has the second least sea ice in the reconstructions while it has a relative large sea ice area in the simulations. This difference could originate from the uncertainty in both our model and the reconstructions, and simulations with more climate models and other reconstructions would be helpful to understand better this model-data discrepancy.

The sea ice variation during the interglacials is strongly coupled with the sea surface temperature and the surface energy budget over the polar oceans (Fig. 5). High surface energy budget leads to warmer sea surface temperature and less sea ice, and vice versa. In both the Arctic and Southern Ocean, the highest surface energy budget at MIS-9 and MIS-5 are explained by their relatively high local summer insolation (Fig. 3a) and high CO_2 concentration (Fig. 3b), which lead to low sea ice area; while the lowest surface energy budget at MIS-13 can be explained by low local summer insolation (Fig. 3a) and low CO_2 concentration (Fig. 3b), which leads to high sea ice area. In addition, the Arctic and Southern Ocean sea ice conditions are also influenced by the variation in the poleward global oceanic meridional heat transport across 60°N and 60°S respectively, although the northward global oceanic meridional heat transport across 60°N is pretty small (Goosse and Renssen 2001; Yin and Berger 2012). The largest southward global oceanic meridional heat transport across 60°S at MIS-5 and MIS-9 (Yin and Berger 2012) could also have contributed to the lowest Southern Ocean sea ice area during the two interglacials (Fig. 2b).

3.2 Comparison of sea ice between the past interglacials and the present

Fig. 6a and Fig. 6b show the annual and seasonal sea ice area anomaly of the last nine interglacials as compared to the PI. In the Arctic, the interglacials all have less annual mean sea ice than the PI, with the maximum sea ice decrease of about 22% at MIS-15 and the minimum decrease of about 11% at MIS-13 (Fig. 6a). For each interglacial, the four seasons all have less sea ice, and the sea ice decrease in summer is much larger than in other seasons. As has been discussed in Sect. 3.1, most variation of the summer Arctic sea ice can be explained by insolation. Moreover, the CO_{2eq} difference between the interglacials and the PI is relatively small, ranging from 4 to 46 ppmv (Fig. 3b). The much less summer sea ice during the interglacials is therefore mainly due to the much higher summer insolation during the past interglacials as compared to the PI (Fig. 3a). Fig. 7 shows the detailed spatial comparison of the summer Arctic sea ice concentration between MIS-15, MIS-13 and the PI. As compared to the PI, the sea ice in the Barents sea, North Greenland sea, Labrador sea and Beaufort sea totally melts, and the sea ice concentration in the central Arctic largely decreases in MIS-15. The sea ice extent at MIS-13 is larger than that at MIS-15, but it still retreats in the Barents sea and North Greenland sea when compared to the PI. In the PMIP simulations of the middle Holocene and the last interglacial, most models have also simulated less Arctic sea ice as compared to the PI due to the intensified summer insolation in the Arctic, and the sea ice anomaly simulated by LOVECLIM is at the middle value among the PMIP simulations (Kageyama et al. 2020; Otto-Bliesner et al. 2021).

In the Southern Ocean, most interglacials have less sea ice than the PI (Fig. 6b), except MIS-13 and MIS-17 which have about 25%-30% more sea ice during local summer and autumn, leading to more annual sea ice. As has been discussed in Sect. 3.1, both insolation and CO_2 play an important role in the summer Southern Ocean sea ice. The much more summer sea ice at MIS-13 and MIS-17 is due to their relatively low CO_2 concentration (Fig. 3b) and low local summer insolation (Fig. 3a). On the contrary, due to high CO_2 concentration (Fig. 3b) and high local summer insolation (Fig. 3a), the sea ice area at MIS-9 is about 25%-30% less than the PI (Fig. 6b). As compared to the PI, the summer Southern Ocean sea ice at MIS-13 noticeably advanced, especially in the west Southern Ocean that it extended to the 60°S; but it significantly retreated at MIS-9, and the retreat is also obvious in the west Southern Ocean (Fig. 7).

As compared to the PI which has a similar CO_2 concentration to many interglacials, the CO_2 concentration of the PD is much larger with an increase of 66 ppmv above the PI level. However, in terms of the comparison with the past interglacials, this larger amount of CO_2 does not make significant difference between the PD ($3.71*10^6$ km^2) and the PI ($3.79*10^6$ km^2) in the Arctic sea ice. This is because the variation of the Arctic sea ice area is mainly controlled by summer insolation as explained in Sect. 3.1, which is the assumed to be the same between the PI and the PD. In the Southern Ocean, the sea ice area in the PD ($3.12*10^6$ km^2) is about 10% less than in the PI ($3.42*10^6$ km^2) due to the increase of CO_2. As a consequence, the sea ice area at MIS-17 and MIS-13, which is already well above the PI level, is even larger when compared to the PD, with an increase of about 50% in local summer and autumn (Fig. 7d). The positive sea ice anomaly at MIS-7 and MIS-15 is also more pronounced when compared to the PD. Compared to the PD, the warm interglacials MIS-5 and MIS-9 still have much less sea ice in the Southern Ocean, with a reduction of about 15% and 20% in the annual mean.

3.3 Comparison of sea ice between interglacials and the future

As compared to the PI, the annual mean Arctic sea ice decreases by about 1.8 10^6 km^2 in the PI_double experiment, a value which is at the low level among the PMIP simulations (Fig. 1), and the south boundary of the sea ice in the North Atlantic largely shifts northward and the sea ice concentration in the central Arctic largely decreases (Fig. 7). In the Southern Ocean, the annual mean sea ice in the PI_double experiment decreases by about 5.6 10^6 km^2 as compared to the PI which is at the high level among the PMIP simulations (Fig. 1). In addition, the sea ice is mainly constrained around the Weddell sea and Ross sea in the PI_double experiment due to the significant decrease (Fig. 7).

It is shown in Sect. 3.2 that as compared to the present-day, all the last nine interglacials have much less sea ice in the Arctic and many also have less sea ice in the Southern Ocean. Fig. 8a shows that, as compared to the PI_double experiment, in the Arctic, all the interglacials still have significantly less sea ice in summer due to much higher summer insolation, with the maximum decrease at MIS-15 and minimum decrease at MIS-13. At MIS-15, the sea ice south boundary in the North Atlantic retreats to the north of 75°N, and sea ice in the Beaufort Sea totally melts when compared to the PI_double (Fig. 7). The sea ice extent at MIS-13 is generally similar to the PI_double, but the sea ice concentration in the central Arctic is significantly less (Fig. 7). On the other hand, there is more sea ice in other seasons for most interglacials due to their much lower CO_2 concentration. In the annual mean, the sea ice area in MIS-5, MIS-9 and MIS-15, which have the highest summer insolation in the northern high latitudes, is still smaller than the future by about 7%, whereas MIS-7, MIS-11, MIS-13 and MIS-17 have more annual sea ice than the future. The annual sea ice area of MIS-1 and MIS-19 is very close to that of the future, which means that in terms of annual sea ice area in the Arctic, the effect of a CO_2 increase of about 295 ppmv is balanced by the effect of an increase of summer insolation at 65°N by 50 W/m^2.

In the Southern Ocean, the interglacials all have much more annual mean sea ice than the future (Fig. 8b), with the MIS-13 maximum annual mean sea ice being about 134% larger and the MIS-9 minimum about 62%. For each interglacial, the four seasons all have more sea ice, and the sea ice increase in summer is the largest (Fig. 8b). This is due to the dominant role of CO_2 on the Southern Ocean sea ice, and the much lower CO_2 concentration during the interglacials than the future.

4. Conclusions

In this study, the sea ice variability of the last nine interglacials, as well as their differences from the present and future are investigated through simulations with the LOVECLIM model. Our results show that the last nine interglacials have different sea ice variations in the Arctic and in the Southern Ocean. In the Arctic, MIS-15, MIS-9 and MIS-5 have the smallest annual mean sea ice area, and MIS-13 has the largest one. The annual mean Arctic sea ice area variation is dominated by the variation in summer, which is mainly controlled by the summer insolation. Thus, the annual mean Arctic sea ice variation during the interglacials is mainly explained by the summer insolation. The annual mean Southern Ocean sea ice variation during the interglacials is mainly explained by the CO_2 concentration, but the effect of insolation can't be ignored. MIS-13 and MIS-17 have the largest annual mean Southern Ocean sea ice area, which is mainly explained by their lowest CO_2 concentration combined with the low local summer insolation. The simulated variations of the Southern Ocean sea ice area of the interglacials are in good consistency with the sea ice reconstructions based on proxy records from the Antarctica ice core.

As compared to the present (both the PI and PD experiments), the interglacials all have less annual mean Arctic sea ice, which is explained by the much higher summer insolation in the

Arctic during the interglacials. As compared to the future, in the Arctic, all the interglacials still have significantly less sea ice in summer due to much higher summer insolation, with the maximum sea ice decrease of about 50% at MIS-15, but there is more sea ice in other seasons for most interglacials due to their much lower CO_2 concentration. In the Southern Ocean, the interglacials all have more both annual mean and seasonal sea ice, which can be explained by the much lower CO_2 concentration, with the maximum annual mean sea ice increase of about 134% at MIS-13.

As far as the potential analogue of our present interglacial is concerned, our results show that MIS-19 is the closest to MIS-1 in terms of the Arctic and Southern Ocean sea ice. However, when compared with the present condition (the PI or PD), the last nine interglacials all show significant differences in the Arctic and Southern Ocean sea ice and in particular show greater seasonal differences. These differences are mainly due to the different seasonal insolation distribution between the intergalcials and the present. Therefore, in the search of potential analogue of the present or future climate, the seasonal climate variations deserve to be considered. Our results show that due to their much higher summer insolation in the Arctic, the last nine interglacials all have much reduced sea ice in the Arctic and therefore could possibly be considered to some degree as analogue for the future in terms of changes in Arctic sea ice. However, it is hard to consider the nine interglacials as analogue for the future in terms of the Southern Ocean sea ice, because they all have much more sea ice than the double CO_2 experiment in the Southern Ocean due to their much lower CO_2 concentration.

Acknowledgments

This work is supported by the Fonds de la Recherche Scientifique-FNRS (F.R.S.-FNRS) under grant MIS F.4529.18 and the National Natural Science Foundation of China (Grant Nos. 41888101 and 41690114). Q.Z. Yin is Research Associate F.R.S.-FNRS. Z.P. Wu thanks Dr. Yurun Tian and Ning Tan for discussion. Computational resources have been provided by the supercomputing facilities of the Université catholique de Louvain (CISM/UCL) and the Consortium des Équipements de Calcul Intensif en Fédération Wallonie Bruxelles (CÉCI) funded by the Fond de la Recherche Scientifique de Belgique (F.R.S.-FNRS) under convention 2.5020.11.

References

Berger AL (1978) Long-term variations of daily insolation and Quaternary climatic changes. J Atmos Sci 35(12):2362-2367. https://doi.org/10.1175/1520-0469(1978)035<2362:LTVODI>2.0.CO;2

Bennike O (2004) Holocene sea-ice variations in Greenland: onshore evidence. Holocene 14(4):607-613. https://doi.org/10.1191/0959683604hl722rr

Cox PM, Huntingford C, Williamson MS (2018) Emergent constraint on equilibrium climate sensitivity from global temperature variability. Nature 553(7688):319-322. https://doi.org/10.1038/nature25450

Cronin TM, Gemery L, Briggs JrWM, Jakobsson M, Polyak L, Brouwers EM (2010) Quaternary Sea-ice history in the Arctic Ocean based on a new Ostracode sea-ice proxy. Quat Sci Rev 29(25-26):3415-3429. https://doi.org/10.1016/j.quascirev.2010.05.024

Cronin TM, Polyak L, Reed D, Kandiano ES, Marzen RE, Council EA (2013) A 600-ka Arctic sea-ice record from Mendeleev Ridge based on ostracodes. Quat Sci Rev 79:157-167. https://doi.org/10.1016/j.quascirev.2012.12.010

Cronin TM, Dwyer GS, Caverly EK, Farmer J, DeNinno LH, Rodriguez-Lazaro J, Gemery L (2017) Enhanced Arctic amplification began at the Mid-Brunhes Event ~400,000 years ago. Sci Rep 7(1):1-7. https://doi.org/10.1038/s41598-017-13821-2

de Vernal A, Hillaire-Marcel C, Le Duc C, Roberge P, Brice C, Matthiessen J, Spielhagen RF, Stein R (2020) Natural variability of the Arctic Ocean sea ice during the present interglacial. P Natl Acad Sci 117(42):26069-26075. https://doi.org/10.1073/pnas.2008996117

Delille B, Vancoppenolle M, Geilfus NX, Tilbrook B, Lannuzel D, Schoemann V, Becquevort S, Carnat G, Delille D, Lancelot C, Chou L, Dieckmann GS, Tison JL (2014) Southern Ocean CO_2 sink: The contribution of the sea ice. J Geophys Res-Oceans 119(9):6340-6355. https://doi.org/10.1002/2014JC009941

Ducklow H, Fraser WR, Meredith MP, Stammerjohn SE, Doney SC, Douglas G (2013) West Antarctic Peninsula: an ice-dependent coastal marine ecosystem in transition. Oceanography 26(3):190-203. http://dx.doi.org/10.5670/oceanog.2013.62

Goosse H, Fichefet T (1999) Importance of ice-ocean interactions for the global ocean circulation: A model study. J Geophys Res-Oceans 104(C10):23337-23355. https://doi.org/10.1029/1999JC900215

Goosse H, Renssen H (2001) A two-phase response of the Southern Ocean to an increase in greenhouse gas concentrations. Geophys Res Lett 28(18):3469-3472. https://doi.org/10.1029/2001GL013525

Goosse H, Brovkin V, Fichefet T, Haarsma R, Huybrechts P, Jongma J, Mouchet A, Selten F, Barriat PY, Campin JM, Deleersnijder E, Driesschaert E, Goelzer H, Janssens I, Loutre MF, Maqueda MAM, Opsteegh T, Mathieu PP, Munhoven G, Pettersson EJ, Renssen H, Roche DM, Schaeffer M, Tartinville B, Timmermann A, Weber SL (2010) Description of the Earth system model of intermediate complexity LOVECLIM version 1.2. Geosci Model Dev 3:603-633. https://doi.org/10.5194/gmd-3-603-2010

Goosse H, Roche DM, Mairesse A, Berger M (2013) Modelling past sea ice changes. Quat Sci Rev 79:191-206. https://doi.org/10.1016/j.quascirev.2013.03.011

Guarino MV, Sime LC, Schröeder D, Malmierca-Vallet I, Rosenblum E, Ringer M, Ridley J, Feltham D, Bitz C, Steig E J, Wolff E, Stroeve J, Sellar A (2020) Sea-ice-free Arctic during the Last Interglacial supports fast future loss. Nat Clim Chang 10(10):928-932. https://doi.org/10.1038/s41558-020-0865-2

Hansen J, Lacis A, Rind D, Russell G, Stone P, Fung I, Ruedy R, Lerner J (1984) Climate sensitivity: analysis of feedback mechanisms. Clim Process Clim Sensit (AGU Geophysical Monograph Series 29), 5(29):130–163.

Hobbs WR, Massom R, Stammerjohn S, Reid P, Williams G, Meier W (2016) A review of recent changes in Southern Ocean sea ice, their drivers and forcings. Glob Planet Chang 143:228-250. https://doi.org/10.1016/j.gloplacha.2016.06.008

IPCC (2014) Climate Change 2014: Synthesis Report. Contribution of Working Groups I, II and III to the Fifth Assessment Report of the Intergovernmental Panel on Climate Change [Core Writing Team, R.K. Pachauri and L.A. Meyer (eds.)]. IPCC, Geneva, Switzerland, 151 pp.

Kageyama M, Sime LC, Sicard M, Guarino MV, de Vernal A, Stein R, Schroeder D, Malmierca-Vallet I, Abe-Ouchi A, Bitz C, Braconnot P, Brady EC, Cao J, Chamberlain MA, Feltham D, Guo CC, LeGrande AN, Lohmann G, Meissner KJ, Menviel L, Morozova PA, Nisancioglu KH, Otto-Bliesner BL, O'ishi R, Buarque SR, y Mélia DS, Sherriff-Tadano S, Stroeve J, Shi XX, Sun B, Tomas RA, Volodin E, Yeung NKH, Zhang Q, Zhang ZS, Zheng WP, Ziehn T (2021) A multi-model CMIP6-PMIP4 study of Arctic sea ice at 127 ka: sea ice data compilation and model differences. Clim Past 17(1):37-62. https://doi.org/10.5194/cp-17-37-2021

Kidston J, Taschetto AS, Thompson DWJ, England MH (2011) The influence of Southern Hemisphere sea-ice extent on the latitude of the mid-latitude jet stream. Geophys Res Lett 38(15):532-560. https://doi.org/10.1029/2011GL048056

Krinner G, Magand O, Simmonds I, Genthon C, Dufresne JL (2007) Simulated Antarctic precipitation and surface mass balance at the end of the twentieth and twenty-first centuries. Clim Dyn 28(2-3):215-230. https://doi.org/10.1007/s00382-006-0177-x

Lo L, Belt ST, Lattaud J, Friedrich T, Zeeden C, Schouten S, Smik L, Timmermann A, Cabedo-Sanz P, Huang JJ, Zhou LP, Ou TH, Chang YP, Wang LC, Chou YM, Shen CC, Chen MT, Wei KY, Song SR, Fang TH, Gorbarenko SA, Wang WL, Lee TQ, Elderfield H, Hodell D A (2018) Precession and atmospheric CO_2 modulated variability of sea ice in the central Okhotsk Sea since 130,000 years ago. Earth Planet Sci Lett 488:36-45. https://doi.org/10.1016/j.epsl.2018.02.005

Myhre G, Myhre CL, Forster PM, Shine KP (2017) Halfway to doubling of CO_2 radiative forcing. Nat Geosci 10(10):710-711. https://doi.org/10.1038/ngeo3036

Nijsse FJMM, Cox PM, Williamson MS (2020) Emergent constraints on transient climate response (TCR) and equilibrium climate sensitivity (ECS) from historical warming in CMIP5 and CMIP6 models. Earth Syst Dynam 11(3):737-750. https://doi.org/10.5194/esd-11-737-2020

Otto-Bliesner BL, Brady EC, Tomas RA, Albani S, Bartlein PJ, Mahowald NM, Shafer SL, Kluzek E, Lawrence PJ, Leguy G, Rothstein M, Sommers AN (2020) A comparison of the CMIP6 midHolocene and lig127k simulations in CESM2. Paleoceanogr Paleocl 35(11):e2020PA003957. https://doi.org/10.1029/2020PA003957

Otto-Bliesner BL, Brady EC, Zhao A, Brierley CM, Axford Y, Capron E, Govin A, Hoffman JS, Isaacs E, Kageyama M, Scussolini P, Tzedakis PC, Williams CJR, Wolff E, Abe-Ouchi A, Braconnot P, Buarque SR, Cao J, de Vernal A, Guarino MV, Guo CC, LeGrande AN, Lohmann G, Meissner KJ, Menviel L, Morozova PA, Nisancioglu KH, O'ishi R, y Mélia DS, Shi XX, Sicard M, Sime L, Stepanek C, Tomas R, Volodin E, Yeung NKH, Zhang Q, Zhang ZS, Zheng WP (2021) Large-scale features of Last Interglacial climate: results from evaluating the lig127k simulations for the Coupled Model Intercomparison Project (CMIP6)-Paleoclimate Modeling Intercomparison Project (PMIP4). Clim Past 17(1):63-94. https://doi.org/10.5194/cp-17-63-2021

Past Interglacials Working Group of PAGES (2016) Interglacials of the last 800,000 years. Rev Geophys 54(1):162-219. https://doi.org/10.1002/2015RG000482

Polyak L, Alley RB, Andrews JT, Grette JB, Cronin TM, Darby DA, Dyke AS, Fitzpatrick JJ, Funder S, Holland M, Jennings AE, Miller GH, O'Regan M, Savelle J, Serreze M, John KS, White JWC, Wolff E (2010) History of sea ice in the Arctic. Quat Sci Rev 29(15-16):1757-1778. https://doi.org/10.1016/j.quascirev.2010.02.010

Renssen H, Goosse H, Fichefet T, Brovkin V, Driesschaert E, Wolk F (2005a) Simulating the Holocene climate evolution at northern high latitudes using a coupled atmosphere-sea ice-ocean-vegetation model. Clim Dyn 24:23-43. https://doi.org/10.1007/s00382-004-0485-y

Renssen H, Goosse H, Fichefet T, Masson-Delmotte V, Koç N (2005b) Holocene climate evolution in the high-latitude Southern Hemisphere simulated by a coupled atmosphere-sea ice-ocean-vegetation model. Holocene 15(7):951-964. https://doi.org/10.1191/0959683605hl869ra

Rugenstein M, Bloch-Johnson J, Gregory J, Andrews T, Mauritsen T, Li C, Frölicher TL, Paynter D, Danabasoglu G, Yang ST, Dufresne JL, Cao L, Schmidt GA, Abe-Ouchi A, Geoffroy O, Knutti R (2020) Equilibrium climate sensitivity estimated by equilibrating climate models. Geophys Res Lett 47(4):e2019GL083898. https://doi.org/10.1029/2019GL083898

Serreze MC, Barry RG (2011) Processes and impacts of Arctic amplification: A research synthesis. Glob Planet Chang 77(1-2):85-96. https://doi.org/10.1016/j.gloplacha.2011.03.004

Serreze MC, Stroeve J, Barrett AP, Boisvert LN (2016) Summer atmospheric circulation anomalies over the Arctic Ocean and their influences on September sea ice extent: A cautionary tale. J Geophys Res-Atmos 121(19):11463-11485. https://doi.org/10.1002/2016JD025161

Stein R, Fahl K, Gierz P, Niessen F, Lohmann G (2017) Arctic Ocean sea ice cover during the penultimate glacial and the last interglacial. Nat Commun 8(1):1-13. https://doi.org/10.1038/s41467-017-00552-1

Timmermann A, Friedrich T, Timm OE, Chikamoto MO, Abe-Ouchi A, Ganopolski A (2014) Modeling obliquity and CO_2 effects on Southern Hemisphere climate during the past 408ka. J Clim 27(5):1863-1875. https://doi.org/10.1175/JCLI-D-13-00311.1

Titchner HA, Rayner NA (2014) The Met Office Hadley Centre sea ice and sea surface temperature data set, version 2:1. Sea ice concentrations. J Geophys Res-Atmos 119(6):2864-2889. https://doi.org/10.1002/2013JD020316

Turner J, Hosking JS, Phillips T, Marshall GJ (2013) Temporal and spatial evolution of the Antarctic sea ice prior to the September 2012 record maximum extent. Geophys Res Lett 40(22):5894-5898. https://doi.org/10.1002/2013GL058371

Tzedakis PC, Raynaud D, McManus JF, Berger A, Brovkin V, Kiefer T (2009) Interglacial diversity. Nat Geosci 2(11):751-755. https://doi.org/10.1038/ngeo660

Tzedakis PC, Channell JET, Hodell DA, Kleiven HF, Skinner LC (2012) Determining the natural length of the current interglacial. Nat Geosci 5(2):138-141. https://doi.org/10.1038/ngeo1358

Vare LL, Massé G, Gregory TR, Smart CW, Belt ST (2009) Sea ice variations in the central Canadian Arctic Archipelago during the Holocene. Quat Sci Rev 28(13-14):1354-1366. https://doi.org/10.1016/j.quascirev.2009.01.013

Wolff EW, Fischer H, Fundel F, Ruth U, Twarloh B, Littot GC, Mulvaney R, Rothlisberger R, de Angelis M, Boutron CF, Hansson M, Jonsell U, Hutterli MA, Lambert F, Kaufmann P, Stauffer B, Stocker TF, Steffensen JP, Bigler M, Siggaard-Andersen ML, Udisti R, Becagli S, Castellano E, Severi M, Wagenbach D, Barbante C, Gabrielli P, Gaspari V (2006) Southern Ocean sea-ice extent, productivity and iron flux over the past eight glacial cycles. Nature 440(7083):491-496. https://doi.org/10.1038/nature04614

Wu ZP, Yin QZ, Guo ZT, Berger A (2020) Hemisphere differences in response of sea surface temperature and sea ice to precession and obliquity. Glob Planet Change 192:103223. https://doi.org/10.1016/j.gloplacha.2020.103223

Yin QZ, Berger A (2010) Insolation and CO_2 contribution to the interglacial climate before and after the Mid-Brunhes Event. Nat Geosci 3(4):243-246. https://doi.org/10.1038/ngeo771

Yin QZ, Berger A (2012) Individual contribution of insolation and CO_2 to the interglacial climates of the past 800,000 years. Clim Dyn 38(3-4):709-724. https://doi.org/10.1007/s00382-011-1013-5

Yin QZ, Berger A (2015) Interglacial analogues of the Holocene and its natural near future. Quat Sci Rev 120:28-46. https://doi.org/10.1016/j.quascirev.2015.04.008

Figures

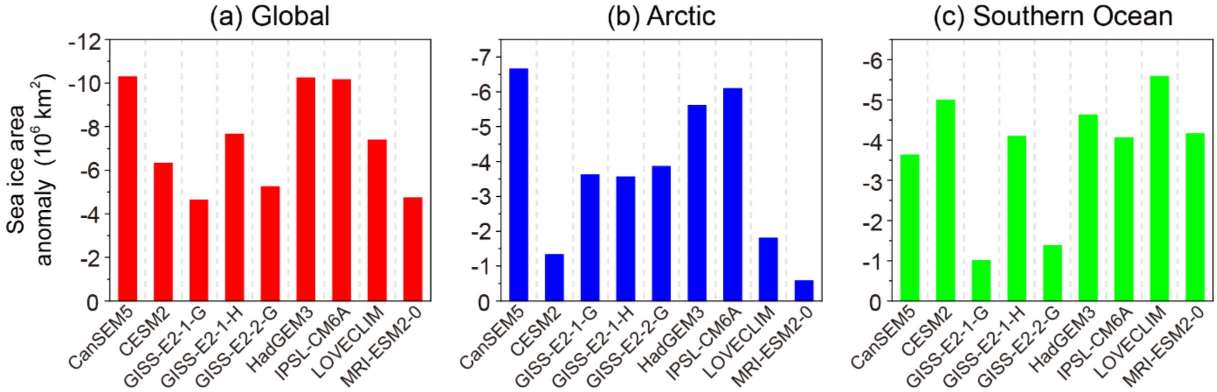

Fig. 1 The sea ice area anomaly of the PI_double experiment relative to the PI experiment simulated by different models for (a) global, (b) Arctic and (c) Southern Ocean. The data of LOVECLIM is from this study and those of other models are from: https://esgf-data.dkrz.de/search/cmip6-dkrz/.

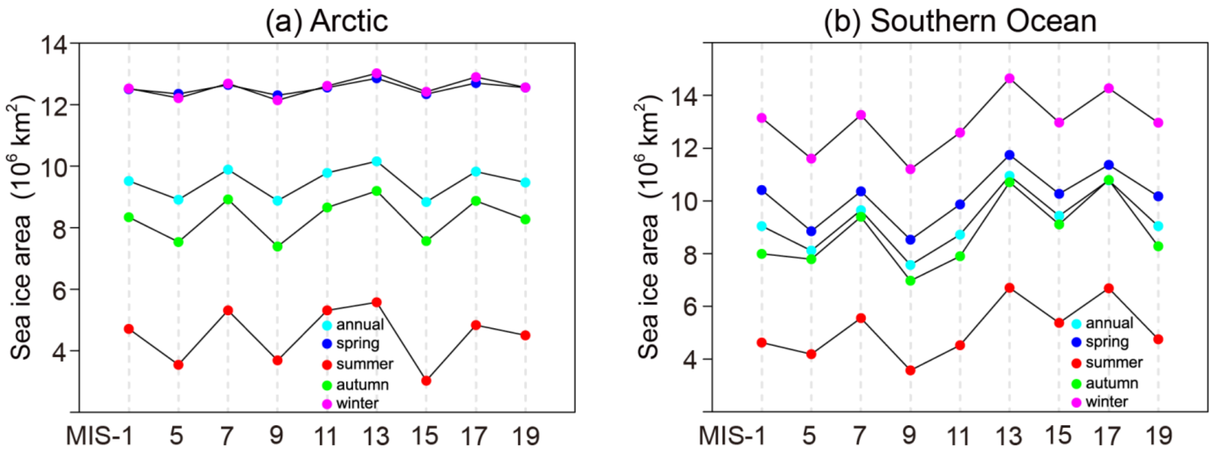

Fig. 2 Simulated annual and seasonal sea ice area during the nine interglacials in the (a) Arctic and (b) Southern Ocean. The seasons refer to the local seasons. Color is usually red for local summer and pink for local winter.

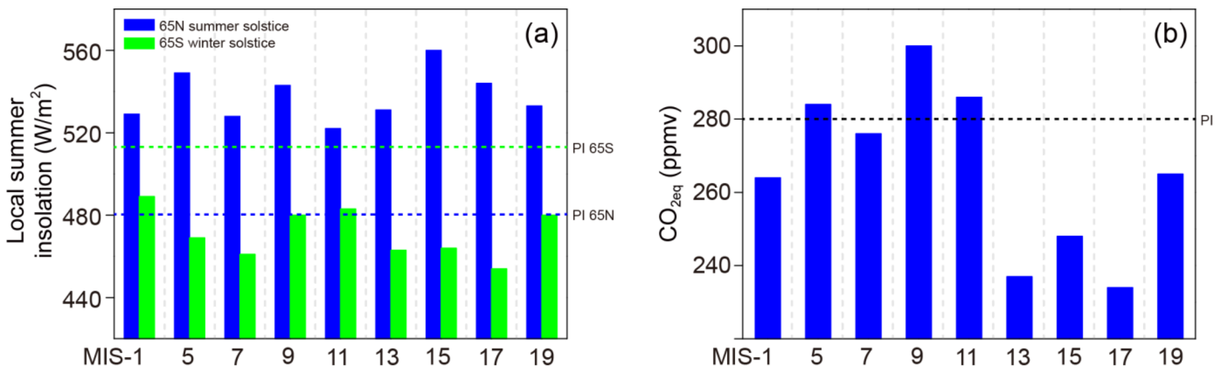

Fig. 3 Local summer insolation at 65°N and 65°S (Berger, 1978) (a) and the CO_{2eq} concentrations (b) during the nine interglacials and the PI.

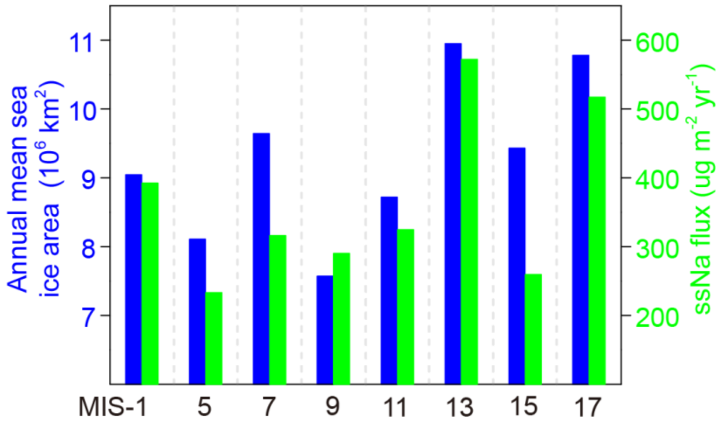

Fig. 4 Simulated annual mean Southern Ocean sea ice area (blue bars) in comparison to the EPICA Dome C sea salt flux (Wolff et al., 2006) (green bars), the minimum values of the EPICA Dome C sea salt flux for each interglacial are used.

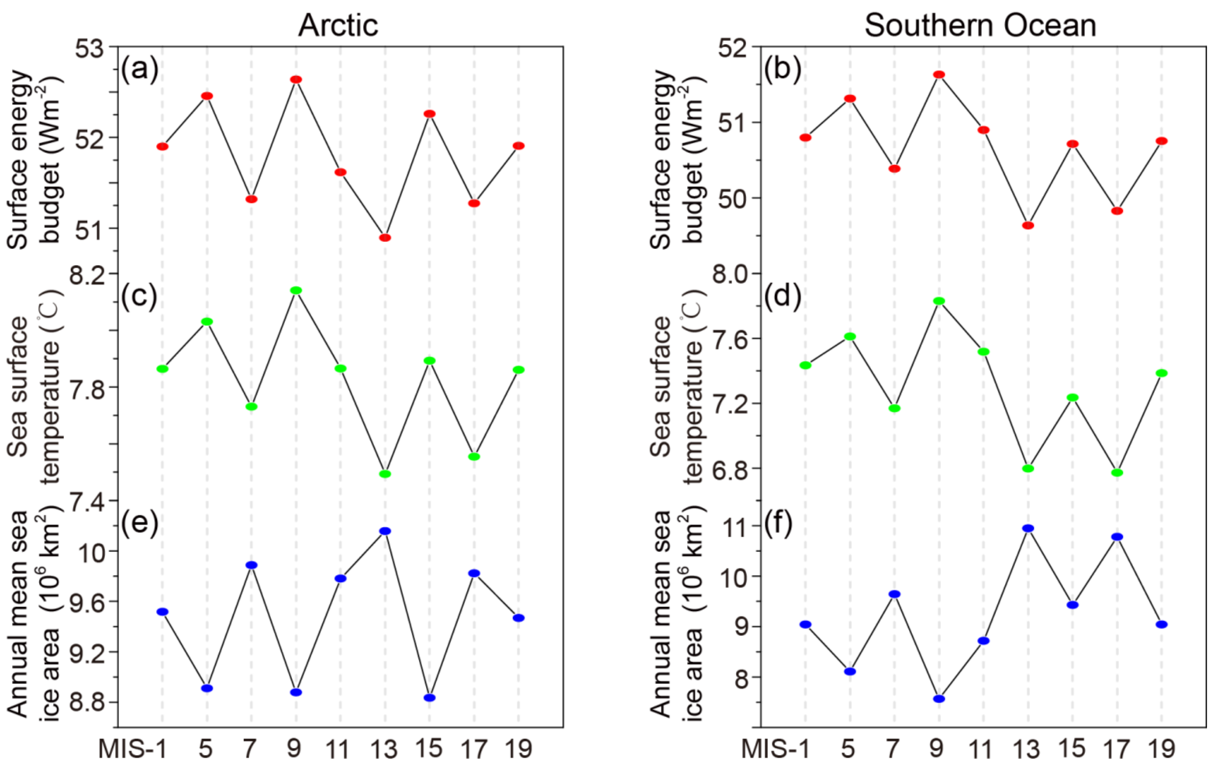

Fig. 5 Annual mean sea ice area, sea surface temperature and surface energy budget over the Arctic (40°N-90°N) and Southern Ocean (40°S-90°S).

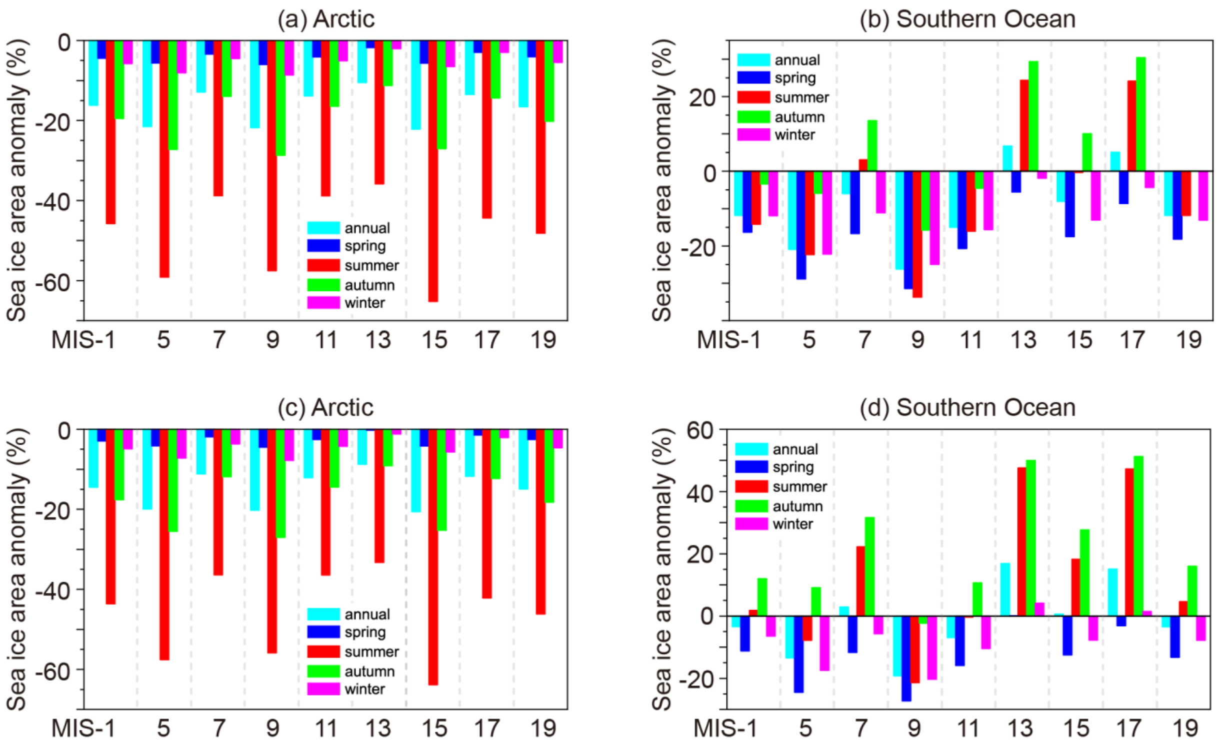

Fig. 6 Annual and local seasonal sea ice area anomaly during the last nine interglacials in the Arctic and Southern Ocean, relative to the PI experiment (a, b) and PD experiment (c, d).

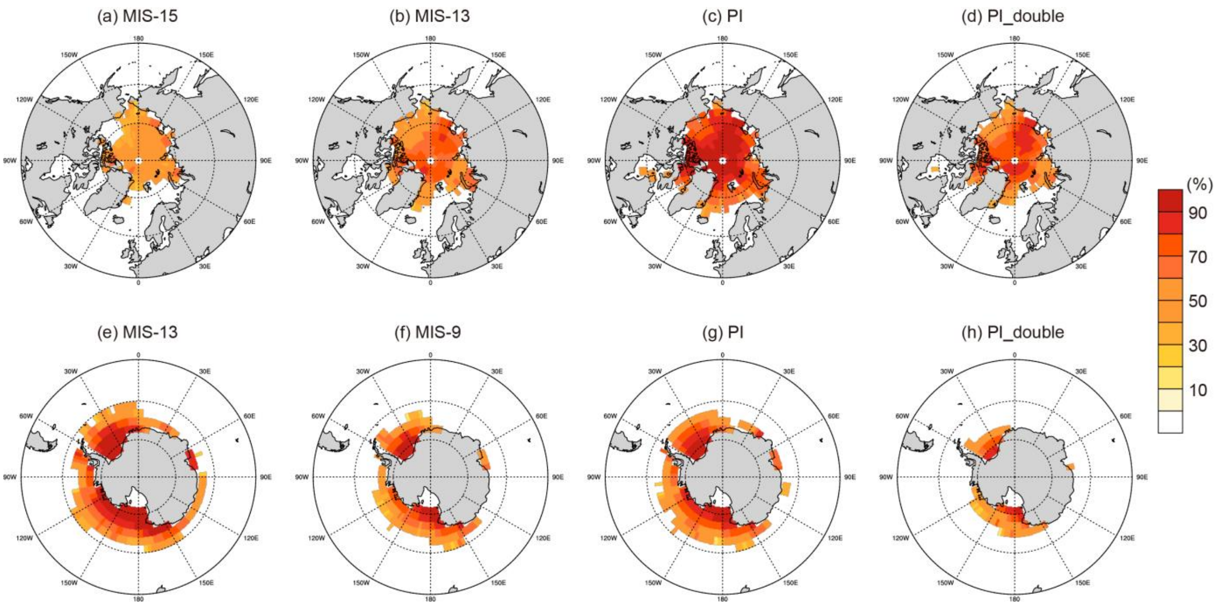

Fig. 7 Simulated summer Arctic sea ice concentration at (a) MIS-15, (b) MIS-13, (c) PI, (d) PI_double and summer Southern Ocean sea ice concentration at (e) MIS-13, (f) MIS-9, (g) PI, (h) PI_double.

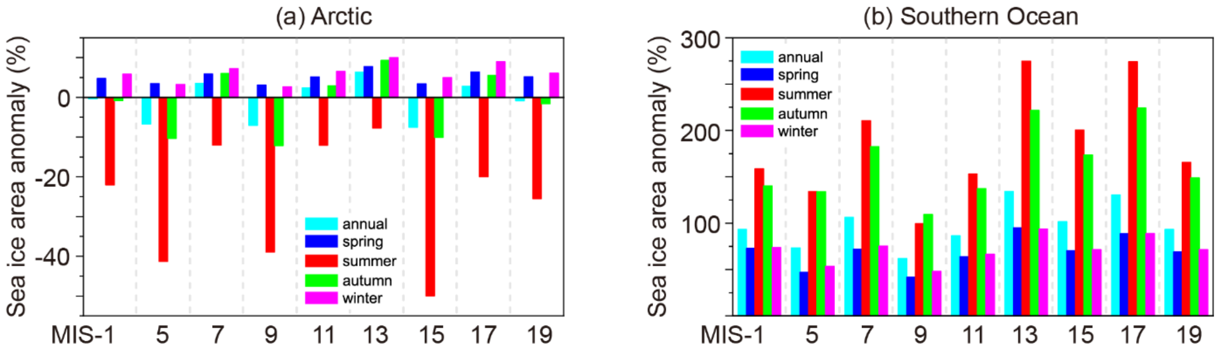

Fig. 8 As compared to the PI_double experiment, annual and local seasonal sea ice area anomaly during the last nine interglacials in the (a) Arctic and (b) Southern Ocean.